Available online at www.sciencedirect.com
SCIENCE DIRECT®
International Journal of Heat and Mass Transfer 47 (2004) 5101–5113
International Journal of HEAT and MASS TRANSFER
www.elsevier.com/locate/ijhmt

The dynamics of spherical bubble growth

A.J. Robinson, R.L. Judd *

Department of Mechanical Engineering, McMaster University, Hamilton, ONT, Canada L8S 4L7

Received 31 December 2003; received in revised form 20 May 2004
Available online 18 August 2004

Abstract

Spherically symmetric bubble expansion in uniformly superheated infinite pools of liquid have been simulated numerically. Bubble growth curves have been generated for a range of Jakob numbers, $3 \leqslant Ja \leqslant 3167$, by altering the initial metastable state of the system facilitated by changes in the initial superheat and system pressure. The detailed physics of vapour bubble growth is studied through delineation of the parameters governing the changes in the growth dynamics from surface tension, to inertia dominated, to diffusion controlled, and the domains between them.

1. Introduction

The progression towards an accurate prediction of the heat transfer rates during nucleate pool boiling is hampered by the seemingly insurmountable task of developing a physical model and solution technique which takes into account all of the factors which significantly influence bubble nucleation, growth and departure. However, in recent times, theories predicting bubble growth have progressed markedly and now provide considerable insight into the nucleate boiling phenomena by exploring the fundamental nature of bubble growth.

The natural starting point for the study of bubble growth during boiling processes is the ideal case of spherically symmetric bubble expansion in a uniformly superheated infinite pool of liquid. Although greatly simplified over the practical case of heating from a solid surface, exact analytic solutions are unattainable because of the complicated thermal and hydrodynamic interaction of the vapour and liquid at the bubble wall, the pressure–temperature dependence of the vapour and the coupling between the liquid momentum and energy equations through the non-linear convection term. The early theoretical works of Rayleigh [1], Plesset and Zwick [2], Forster and Zuber [3] and Scriven [4], among others, yielded approximate solutions for the bubble growth rate by considering the two limiting regions; the *inertia* and *diffusion* controlled growth regions. Inertia controlled growth is restricted to the initial stages of expansion during which the rate at which the bubble grows is primarily determined by its ability to accelerate or 'push back' the surrounding liquid independent of the rate of vapour generation into the bubble. For this case then, the bubble growth could be predicted by the solution to the momentum equation alone. Assuming potential flow, integration of the one-dimensional momentum equation in the liquid provides an expression which describes the growth of the vapour bubble [2–5] according to

$$\frac{P_v(T_v) - P_\infty}{\rho_l} = R\frac{d^2R}{dt^2} + \frac{3}{2}\left(\frac{dR}{dt}\right)^2 + \frac{2\sigma}{\rho_l R}, \tag{1}$$

where the pressure rise across the vapour–liquid interface has been related by the Young–Laplace equation, $P_v(t) - P_\infty = 2\sigma/R(t)$. Eq. (1), known as the extended or modified Rayleigh equation, is an equilibrium balance between the pressure of the vapour, the surface tension stresses and the net pressure imposed by the liquid. Integration of Eq. (1), assuming the vapour pressure is nearly constant at $P_v \approx P_{sat}(T_\infty)$ and the bubble is large

* Corresponding author. Tel.: +1-905-525-9140; fax: +1-905-572-7944.
E-mail address: juddr@mcmaster.ca (R.L. Judd).

0017-9310/$ - see front matter © 2004 Elsevier Ltd. All rights reserved.
doi:10.1016/j.ijheatmasstransfer.2004.05.023

Nomenclature

C_p	specific heat (J/kg K)
h_{fg}	latent heat of evaporation (J/kg)
Ja	Jakob number, $Ja = \frac{\rho_l C_l (T_\infty - T_{sat}(P_\infty))}{\rho_v h_{fg}}$
M	number of grid points
P	pressure (Pa)
r	radial direction (m)
R	bubble radius (m)
R^+	dimensionless radius in MRG solution
R_c	initial bubble radius (m)
t	time (s)
t^+	dimensionless time in MRG solution
T	temperature (°C)
u	radial velocity (m/s)

Greek symbols

α	thermal diffusivity (m^2/s)
δ	thermal layer thickness (m)
η	transformed computational coordinate, $\eta = \frac{1}{M-1}$
μ	viscosity (kg m/s)
ρ	density (kg/m^3)
σ	surface tension (N/m)

Subscripts

l	liquid
sat	saturation condition
v	vapour
w	wall
∞	far field

enough that the surface tension term is negligible yields the Rayleigh solution for inertial controlled growth

$$R(t) = \left(\frac{2}{3}\left[\frac{T_\infty - T_{sat}(P_\infty)}{T_{sat}(P_\infty)}\right]\frac{h_{fg}\rho_v}{\rho_l}\right)^{1/2} t, \quad (2)$$

where the linearized form of the Clapeyron equation is substituted to relate the saturated vapour temperature and pressure. The existence of the inertial controlled growth stage and corresponding linear relationship has been confirmed by the low pressure experiments of Lien [6] as well as the low pressure numerical simulations of Lee [7] and Robinson [8].

Plesset and Zwick [2], Forster and Zuber [3] and Scriven [4] are foremost among the researchers who extended bubble growth predictions beyond the inertial controlled growth region by taking into account the fact that as the bubble grows, the latent heat requirement of evaporation depletes the energy stored within the superheated layer which has formed at the surface of the bubble. As the bubble grows, its equilibrium vapour temperature decreases from T_∞ to its minimum value of $T_{sat}(P_\infty)$. As the interfacial temperature and corresponding pressure drop, bubble growth becomes limited by the relatively slower diffusion of heat to the vapour–liquid interface, causing the growth rate to continually decrease. Plesset and Zwick [2] and Forster and Zuber [3] obtained analytic solutions which predict the instantaneous bubble radius for thermal diffusion controlled growth by supplying approximate expressions for the temperature of the liquid at the interface and assuming that the thickness of the thermal boundary layer surrounding the bubble is much smaller than the radius of the bubble. The 'thin thermal boundary layer' assumption resulted in expressions for the liquid temperature at the moving interface that took into account the effect of the changing interfacial area on the temperature distribution at the interface [5]. The leading order approximation for the growth rate is given by

$$R(t) = 2CJa\left(\frac{\alpha_l t}{\pi}\right)^{1/2}, \quad (3)$$

where, the constant is $C = (3)^{1/2}$ for Plesset and Zwick [2] and $C = \pi/2$ for Forster and Zuber [3]. The solution for the temperature gradient at a stationary plane interface of a semi-infinite medium gives $C = 1.0$ and Riznic et al. [5] correctly pointed out that the coefficient, C, accounts for the influence of the increasing interfacial area on the temperature gradient near the interface. Eq. (3) was shown to agree very well with the experimental data of Dergarabedian [9] for bubble growth in water at atmospheric pressure and superheats not exceeding 5.1 °C.

Scriven [4] considered thermal diffusion controlled growth without the assumption of a thin thermal boundary layer. By obtaining exact solutions of the equation of energy flow including radial convection, the asymptotic relation of the exact form given by Plesset and Zwick [2] was obtained for the limiting case of moderate to high superheats for commonly used fluids. This result implies that for large enough Jakob number, the thin thermal boundary layer assumption is valid. For commonly used fluids at low superheats, or small Jakob numbers, Scriven [4] obtained an expression which simplifies to

$$R(t) = (2Ja\alpha_l t)^{1/2}. \quad (4)$$

It is noticed that this expression has the same asymptotic dependence on time as Eq. (3) but a different dependence on the Jakob number which implies the thin thermal boundary layer assumption may no longer be valid for

small Jakob numbers. The dependence on the Jakob number expressed in Eqs. (3) and (4) was later confirmed by Riznic et al. [5] who included the influence of interface curvature on the temperature gradient near the interface. In this analytical work two limiting growth rate solutions were determined. For $Ja > 2$, bubble growth was found to be in agreement with Eq. (3), suggesting that the effect of interface curvature was negligible and that the thin thermal boundary layer assumption is valid. For small Jakob numbers ($Ja < 2$), Riznic et al. [5] found that the radius varies according to Eq. (4), leading to the conclusion that for small Jakob number, the thin thermal boundary layer assumption is not valid and curvature of the interface plays an important role.

A complete description of the bubble growth process should be represented by a smooth transition between the early inertia dominated growth and the later diffusion controlled growth. Mikic et al. [10] obtained an expression for the variation of bubble radius with time which spans both regions by interpolating between the limiting solutions for large and small times given by Eqs. (2) and (3), respectively. The expression is often referred to as the MRG solution and is given in the form of scaled radius and time variables

$$R^+ = \frac{2}{3}\left[(t^+ + 1)^{3/2} - (t^+)^{3/2} - 1\right], \tag{5}$$

where the scaled variables are given by

$$R^+ = \frac{RA}{B^2}, \quad t^+ = \frac{tA^2}{B^2}, \quad B = \left(\frac{12\alpha_l}{\pi}\right)^{1/2} Ja,$$
$$A^2 = \frac{2h_{fg}\rho_v[T_\infty - T_{sat}(P_\infty)]}{3\rho_l T_{sat}(P_\infty)}. \tag{6}$$

Because the exact conditions on both ends were built in during the derivation of Eq. (5), the expression approaches Eq. (2) at small times and is asymptotic to Eq. (3) as time approaches infinity. This theory was found to be in good agreement with the experimental data of Lien [6] for water over a wide range of system pressures, including low pressure data with a significant inertia controlled region. The use of the Plesset and Zwick [2] solution in the interpolation formulation confines the applicability of the MRG solution to moderate to high Jakob numbers in which the thin thermal boundary layer assumption is valid [5,11]. Prosperetti and Plesset [11] extended the range of applicability of the MRG type interpolation formula by introducing scaling variables which describe growth over a wider range of superheats.

Although interpolation formulas bridge the gap between the two limiting regimes and provide simple equations for the approximation of the growth characteristics, they are not solutions to the governing equations. As a result, the detailed physics of bubble growth during the transition between the two limits are difficult to interpret. Furthermore, a complete description of bubble growth must include the regime where surface tension forces dominate, which has not been considered in the analytic works above. To address issues such as these, numerical computations of vapour bubble growth in an infinite, uniformly superheated liquid have been performed by Theophanous et al. [12], Judd [13], Board and Duffy [14], Donne and Farranti [15], Lee [7], Lee and Merte [16] and Robinson [8]. In the first three works cited here, the approach was to assume the shape of the temperature profile within the thermal boundary layer which exists around the growing bubble so that the temperature gradient at the vapour–liquid interface could be deduced. The latter four works increased the accuracy of the analysis by numerically solving the one dimensional energy equation in a moving medium. In doing so, the temperature gradient in the liquid at the vapour–liquid interface was obtained from the computed temperature field. By including the necessary parameters in the physical modelling of the problem, a more precise description of the nature of bubble growth is possible. In the present investigation the detailed physics of spherical bubble growth is explored with particular focus on the interaction between the hydrodynamics and the heat transfer near the vapour–liquid interface and their relation to changes in the growth characteristics as the bubble grows through the surface tension, transition and heat transfer domains.

2. Present one-dimensional theory

Allowing for viscous stresses, Eq. (1) requires the term $\frac{4\mu_l(dR/dt)}{\rho_l R}$ on the right hand side. Throughout the parameter space of this investigation, the viscous term is negligible compared with the other stress terms so that potential flow in the liquid can be assumed. Consequently, the equation of motion for the spherical bubble of radius, R, is approximated by the extended Rayleigh equation, Eq. (1). The initial bubble radius is determined by assuming that the vapour is initially saturated with $T_v = T_\infty$ and that it exists in unstable equilibrium with the quiescent surroundings. The critical radius is predicted by the Young–Laplace equation

$$R_c = \frac{2\sigma}{P_{sat}(T_\infty) - P_\infty}. \tag{7}$$

Considering an energy balance at the vapour–liquid interface, the energy required to evaporate the liquid is supplied by thermal diffusion through the liquid. For a spherical bubble this gives

$$\rho_v h_{fg} \frac{dR}{dt} + h_{fg} \frac{R}{3} \frac{d\rho_v}{dt} = \frac{1}{4\pi R^2} \int_{A_s} k_l \left(\frac{\partial T}{\partial R} \right)_{r=R} dA. \quad (8)$$

The temperature gradient at the vapour–liquid interface is obtained by numerically solving the one-dimensional energy equation in spherical coordinates for the moving liquid

$$\frac{\partial T}{\partial t} + u \frac{\partial T}{\partial r} = \alpha_l \left(\frac{\partial^2 T}{\partial r^2} + \frac{2}{r} \frac{\partial T}{\partial r} \right) \quad (9)$$

with initial and boundary conditions given by

$$T(r,0) = T_\infty, \quad T(R,t) = T_v, \quad T(R_\infty,t) = T_\infty. \quad (10)$$

The initial condition states that the entire temperature field in the liquid is constant. The first boundary condition assumes that the temperature of the liquid at the interface is identical to the temperature of the vapour. The far field boundary condition is assumed to be uniform and equal to the initial temperature. The radial velocity is determined as a function of the instantaneous bubble radius and interface velocity by assuming that the flow field can be determined by the solution for irrotational flow around the expanding sphere in an unbounded liquid. The local velocity becomes

$$u(R,t) = \frac{dR}{dt} \left(\frac{R}{r} \right)^2. \quad (11)$$

Finally, it is postulated that the vapour is saturated and remains in thermodynamic equilibrium throughout the growth period so that the pressure and density can be specified as functions of the saturated vapour temperature. As in other works such as Lee [7], the property variations with temperature are obtained from best-fit correlations with available property data.

2.1. Solution procedure

Specifying the vapour density and pressure as functions of the vapour temperature effectively reduces the problem to that of determining the instantaneous values of R, dR/dt and T_v. In order to do so, the following variables are defined,

$$y_1 = T_v, \quad y_2 = R, \quad y_3 = \frac{dR}{dt}. \quad (12)$$

The governing equations were rearranged such that a system of three simultaneous ordinary differential equations resulted

$$\frac{dy_1}{dt} = \frac{dT_v}{dt} = f_1(t, y_1, y_2, y_3),$$
$$\frac{dy_2}{dt} = \frac{dR}{dt} = f_2(t, y_3), \quad \frac{dy_3}{dt} = \frac{d^2R}{dt^2} = f_3(t, y_1, y_2, y_3). \quad (13)$$

For a given time step Δt, the solution of the above system of equations requires that the values y_1, y_2 and y_3 be known at the beginning of the time interval. A fourth-order Runge Kutta scheme was then implemented to determine the updated values.

The energy equation at each time step was solved numerically on a grid which was constructed using a variant of the grid generation technique used by Chen et al. [17]

$$r_j = R + (R_\infty - R) \times \left(1 - S_R \tan^{-1} \left[\left(1 - \frac{j-1}{M-1} \right) \tan \left(\frac{1}{S_R} \right) \right] \right), \quad (14)$$

where S_R determines the percentage of grid points near the interface and has been kept constant at 0.65 throughout this investigation. In order that conventional finite difference techniques could be utilized, the energy equation was transformed into a stationary grid with uniform grid spacing where the spatial and temporal derivatives are related to the metric, r_η, and Jacobian, J, through

$$T_r = J^{-1} r_\eta T_\eta, \quad T_t = T_\tau - T_r r_\tau, \quad (15)$$

where the subscripts denote differentiation and η and τ are the new spatial and temporal coordinates, respectively. The transformed energy equation becomes

$$T_\tau + a T_\eta + b T_{\eta\eta} = 0. \quad (16)$$

The Jacobian and the coefficients a and b are related to the metric and its derivative through

$$J = r_\eta^2, \quad a = \frac{U^c}{J} + \frac{\alpha_l r_\eta r_{\eta\eta}}{J^2} - \frac{2\alpha_l r_\eta}{Jr}, \quad b = \frac{\alpha_l r_\eta^2}{J^2}. \quad (17)$$

Equation (16) was discretized using second order central difference representations of the spatial derivatives and a fully implicit first order representation of the time derivatives. At a given time step the temperature field was determined by solving the resulting system of algebraic expressions with the Tri-Diagonal Matrix Algorithm (TDMA).

The appropriateness of the physical modelling of the problem and the accuracy of the numerical solution has been assured by rigorous sensitivity studies, including but not limited to grid independence, time step independence and the affect of the initial disturbance required to commence growth from the initial unstable equilibrium state as detailed in Robinson [8]. Agreement with the MRG solution together with some experimental measurements is shown in Figs. 1 and 2, respectively. It must be noted that the delay time, which is the time interval between the disturbance and the time at which the bubble undergoes significant growth, varies depending on the magnitude of the initial disturbance

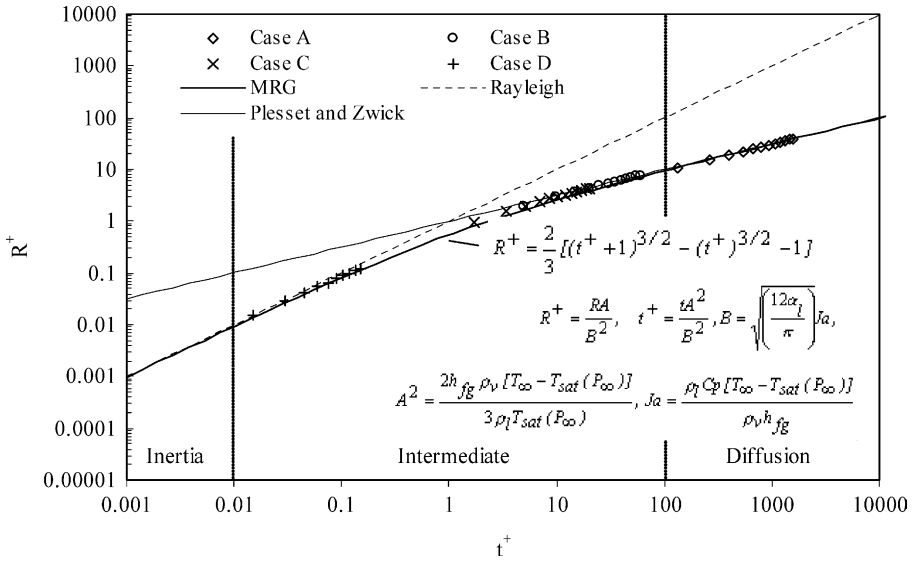

Fig. 1. Comparison of the present solutions with the analytical solution of Mikic et al. [10]. The system conditions correspond with: Case A, water $P_\infty = 1.0$ atm, $\Delta T_{sup} = 3.1$ °C; Case B, water $P_\infty = 0.372$ atm, $\Delta T_{sup} = 6.3$ °C; Case C, water $P_\infty = 0.362$ atm, $\Delta T_{sup} = 17.0$ °C; Case D, R113 $P_\infty = 0.0361$ atm, $\Delta T_{sup} = 48.1$ °C.

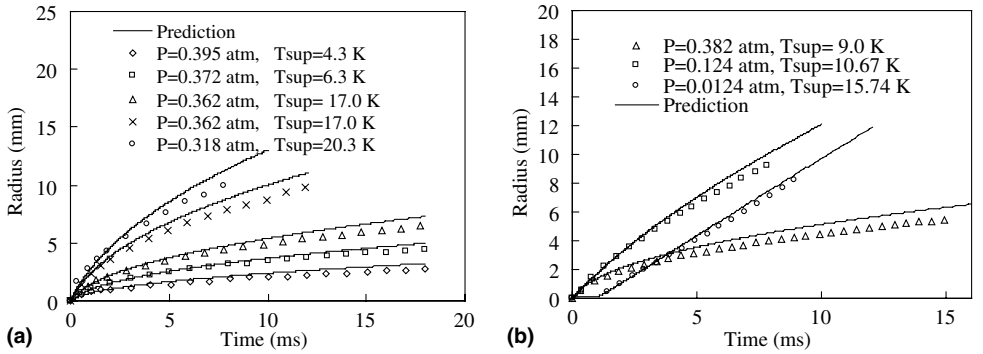

Fig. 2. Comparison of the present numerical analysis with the experimental measurements of (a) Board and Duffy [14] and (b) Lien [6].

[7,8]. For each case tested, a larger disturbance causes the delay time to decrease. However, within a significant range of the disturbance parameters, differences are small enough to be of little practical interest. For this study, growth was initiated with a 0.0005% increase in the critical radius over a time interval of 10^{-9} s. A comprehensive discussion on the effects of varying the disturbance parameters can be found in Lee [7].

3. Spherically symmetric bubble growth dynamics

In the following sections, the fundamental nature of bubble growth is explored by considering the dynamic coupling between the heat transfer and the fluid dynamics in the immediate vicinity of an expanding bubble. The analysis is similar to that advanced by Robinson and Judd [18] for bubble growth near a heated surface, although for the much simpler scenario of spherically symmetric bubble growth. The position taken here is that the instantaneous rate of heat transfer to the bubble interface dictates the growth rate since $dR/dt \propto k_l(\partial T/\partial r)_{r=R}$. However, changes in the rate of heat transfer can be affected significantly by the hydrodynamic resistance of the surrounding liquid. To clarify this concept, two simplifications are made in the following analysis. First, since compressibility effects have been shown to be negligible [8], the interfacial heat flux and the bubble growth rate are analogous and related through

$$\frac{dR}{dt} \approx \frac{1}{\rho_v h_{fg}} \left(k_l \frac{\Delta T(t)}{\delta(t)} \right), \tag{18}$$

where $\Delta T(t) = T_\infty - T_v(t)$ is the effective driving temperature difference of heat transfer and $\delta(t) = \Delta T(t)/(T(t)/\partial r)_{r=R(t)}$ is the extrapolated thickness of the thermal boundary layer surrounding the bubble which is analogous to the thermal resistance to heat transfer. Secondly, the hydrodynamic forces acting at the vapour–liquid interface can be represented by [18]

$$P_{hd} = \rho_l R \frac{d^2R}{dt^2} + \rho_l \frac{3}{2} \left(\frac{dR}{dt} \right)^2. \tag{19}$$

Therefore, pressure exerted by the liquid at the interface is related to the static and hydrodynamic components, $P_l(R) = P_\infty + P_{hd}$.

3.1. Bubble growth for an intermediate Jakob Number, $Ja = 45$

In the following sections, the growth characteristics of a single isolated spherical bubble expanding in a uniformly superheated unbounded liquid will be discussed. The liquid chosen is water and the boiling condition selected is atmospheric pressure at an initial superheat of $\Delta T_{sup} = 15$ °C with a corresponding Jakob number of $Ja = 45$.

3.1.1. Surface tension controlled growth

The surface tension controlled domain occurs immediately after the commencement of bubble growth and ends when the interfacial acceleration is at its maximum. Fig. 3 indicates that during this domain, the growth rate is positive and increasing but that increases in radius are miniscule. Furthermore, Fig. 4 shows that, initially, the hydrodynamic pressure term is insignificant such that Eq. (1) reduces to $\Delta P_v(t) = P_v(t) - P_\infty \approx 2\sigma/R$. Since P_∞ is constant, the inverse relation with radius dictates that even a minute increase in the radius must correspond with a decrease in the vapour pressure, with a proportional drop in the vapour temperature, $T_v(t)$. This effect is significant because, as indicated in Fig. 5, the drop in $T_v(t)$ corresponds to an increasing driving potential, $\Delta T(t)$, with negligible changes in the thermal resistance, $\delta(t) = \delta_0$. This establishes a thermal feedback effect which is responsible for the dramatic increase in bubble acceleration, d^2R/dt^2, shown in Fig. 3. Bubble growth is accelerated since an increasing radius is related to an increase in the driving temperature difference, $\Delta T(t)$ which causes an increase in the rate of thermal diffusion to the vapour–liquid interface through the increase in the magnitude of the local temperature gradient, $(\sim \Delta T(t)/\delta_0)$, which feeds back by a proportional increase in the bubble growth rate, dR/dt via Eq. (18).

In the earlier stage of the surface tension domain ($t < 0.002$ ms), the system is very near the initial equilibrium state. Here, the temperature differential is of the order $O(\Delta T) \sim 10^{-6}$ °C which is still small enough that the expansion rate, and corresponding interface acceleration, are both small as compared with the maximum values shown in Fig. 3. Even still, minute changes in the bubble radius are sufficient to continually cause the temperature difference, $\Delta T(t)$, to escalate as the surface tension stresses are relaxed causing $\Delta P_v(t)$ to decrease. At approximately $t = 0.002$ ms, $d(\Delta T)/dt$ increases

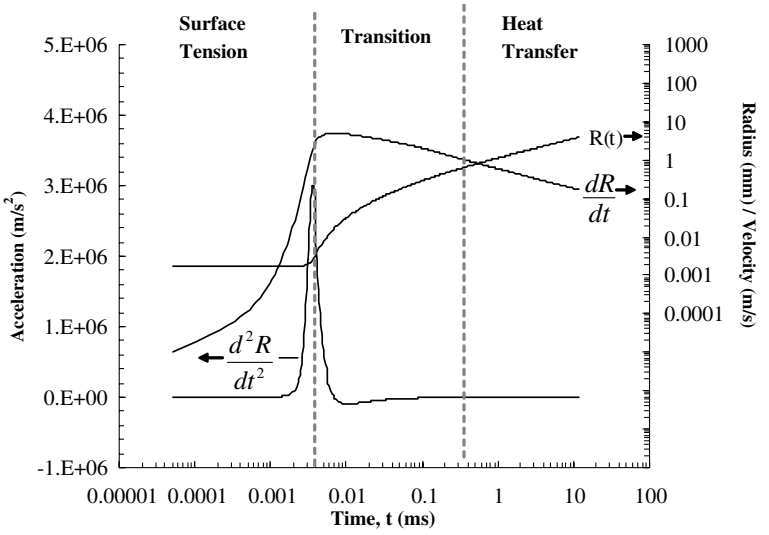

Fig. 3. Bubble growth characteristics for water with ambient conditions $P_\infty = 1.0$ atm, $\Delta T_{sup} = 15$ °C.

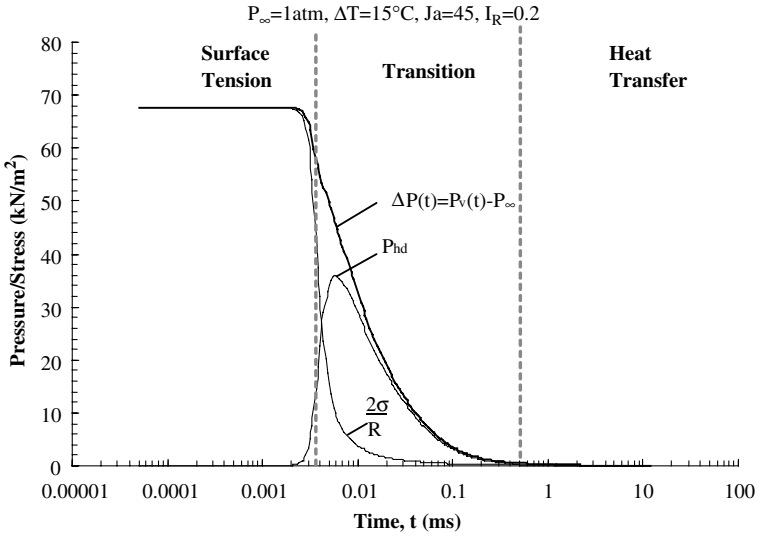

Fig. 4. Bubble growth hydrodynamics for water with ambient conditions $P_\infty = 1.0$ atm, $\Delta T_{sup} = 15$ °C.

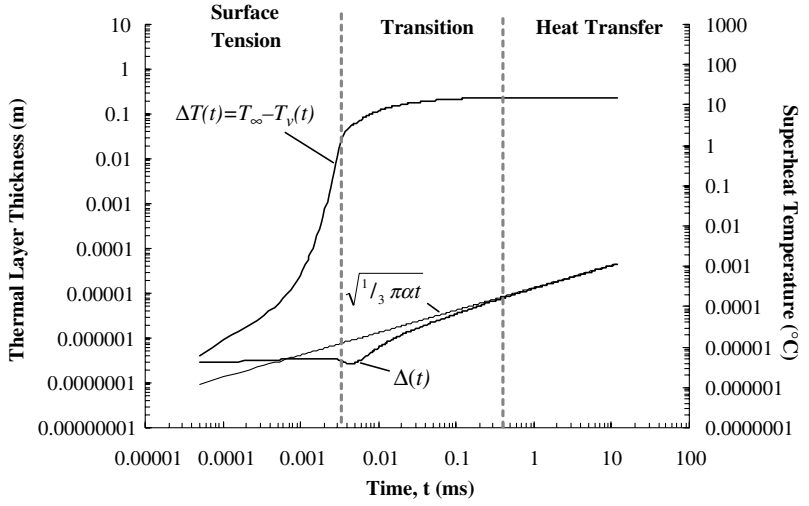

Fig. 5. Bubble growth heat transfer characteristics for water with ambient conditions $P_\infty = 1.0$ atm, $\Delta T_{sup} = 15$ °C.

dramatically as a direct consequence of the thermal feedback effect. In a relatively short time interval ($0.002 \text{ ms} \leqslant t \leqslant 0.0036$ ms), the driving temperature difference increases from nearly zero to almost 2 °C, which is significant. Fig. 3 shows that over the same time interval, the interface undergoes a dramatic increase in acceleration. This is to be expected, since for constant $\delta(t) = \delta_0$, the magnitude of the acceleration is proportional to the time rate of change of $\Delta T(t)$ through the expression

$$\frac{d^2R}{dt^2} \propto \frac{1}{\delta_0}\frac{d(\Delta T)}{dt}. \tag{20}$$

The peak value of the acceleration occurs at $t = 0.0036$ ms and corresponds with the maximum rate of change of $\Delta T(t)$. As shown in Fig. 5, the slope of $\Delta T(t)$ decreases after $t = 0.0036$ ms. This is the point of maximum acceleration and the time that the surface tension controlled growth domain is considered to end.

3.1.2. Transition domain

If left unrestrained, the thermal feedback effect would drive the interfacial heat flux and growth rate up at a fantastic rate, causing the bubble radius to increase several orders of magnitude virtually instantaneously. This is counter intuitive and in fact does not occur

because of the restraining influence that the hydrodynamics have on bubble expansion during the transition domain.

At the beginning of the transition region, the interface acceleration is near the maximum value of $d^2R/dt^2 \approx 3 \times 10^6$ m/s^2, after which the magnitude of the acceleration begins to diminish continually, becoming zero at approximately $t = 0.0068$ ms where the maximum velocity occurs as seen in Fig. 3. The fact that the interface acceleration is decreasing indicates that there are mechanisms at work which tend to depress the aforementioned thermal feedback effect. The most obvious is the fact that the expanding bubble now faces the additional resistance associated with forcing the bulk liquid out radially. The hydrodynamic pressure term rises sharply to become a significant term in the equation of motion and is responsible for a noticeable decrease in the rate at which the pressure difference $\Delta P_v(t)$ is decreasing as shown in Fig. 4 for $t > 0.004$ ms. Because changes in vapour pressure are analogous to changes in vapour temperature, the introduction of the hydrodynamic force at the bubble interface has a detrimental effect on the rate at which the temperature difference $\Delta T(t)$ increases, thus depressing the thermal feedback effect. This is the mechanism which is responsible for the observed decrease in the slope of $\Delta T(t)$ in Fig. 5. Since $d(\Delta T)/dt$ is decreasing and $\delta(t)$ does not change significantly, the magnitude of the acceleration must decrease as predicted by Eq. (10) and shown in Fig. 3 for the time interval $0.0036 \text{ ms} \leqslant t \leqslant 0.0068$ ms.

After $t = 0.0068$ ms the pressure difference, $\Delta P_v(t)$, is primarily balanced by the hydrodynamic pressure at the interface, and the interface acceleration is negative as shown in Figs. 3 and 4, respectively. Fig. 5 indicates that the rate of change of $\Delta T(t)$ continually decreases, approaching zero, as it approaches the system superheat, $\Delta T_{sup} = 15$ °C. However, this alone does not explain why the heat flux is decreasing in magnitude causing bubble expansion to decelerate. As pointed out by Robinson and Judd [18], the heat flux and growth rate are decreasing because the positive influence that increasing $\Delta T(t)$ tends to have on the heat flux is more than offset by the rate at which advection and conduction serve to decrease the temperature gradient at the interface by thickening the thermal boundary layer surrounding the bubble. Because there is significant fluid motion directed radially outward from the expanding interface, the cooler liquid from within the thermal layer penetrates deeper into the bulk of the liquid by advection. This, coupled with a net loss of thermal energy by conduction heat transfer out of the liquid and into the vapour bubble, causes the maximum temperature within the boundary layer to move further out from the bubble interface. Fig. 5 illustrates that this portion of the transition region is identified by considerable growth of the thermal layer. Before this time, the thermal layer thickness remained more or less constant at $\delta(t) \approx 3 \times 10^{-7}$ m. During this stage, however, the boundary layer has grown by nearly two orders of magnitude, $\delta(t = 0.2 \text{ ms}) \approx 8.0 \times 10^{-6}$ m.

3.1.3. Heat transfer controlled growth

Heat transfer controlled growth refers to the interval of bubble growth during which the rate of bubble expansion is limited by the rate at which liquid is evaporated into the bubble, dictated by the rate of heat transfer through the liquid to the interface. In this domain, the pressure difference $\Delta P_v(t)$ has reduced to nearly zero as indicated in Fig. 4. As a result, liquid inertia and surface tension have a negligible influence on bubble growth because the rate at which $\Delta P_v(t)$ decreases no longer has a significant bearing on the rate at which the driving temperature difference $\Delta T(t)$ increases since it is approximately constant at 15 °C according to Fig. 5. Consequently, the growth characteristics of this domain are determined solely by the increased thermal resistance associated with the growing thermal boundary layer. Fig. 5 shows that the extrapolated thermal boundary layer thickness increases steadily with no significant change in $\Delta T(t)$. Also shown in the figure is the analytic expression for the thermal boundary layer thickness determined by Plesset and Zwick [2] for a thin thermal boundary layer assumption, $\delta(t) = (1/3\pi\alpha t)^{1/2}$. The close agreement confirms the correctness of the both the numerical and analytic solutions as well as the appropriateness of using the extrapolated thermal boundary layer thickness, $\delta(t)$, for characterizing the thermal resistance in the present analysis.

3.2. The effect of the initial state of the system on the bubble growth dynamics

3.2.1. Effect of system properties on surface tension domain

The initial state of the system establishes the length of the *delay time* as well as the magnitude of the maximum interfacial acceleration. The delay time is significant because it defines the interval between the initiation of growth and the point of maximum acceleration at which the bubble begins to grow significantly away from R_c. The maximum acceleration is also important because the rate of growth at the end of the surface tension domain sets the stage for the growth characteristics of the transition domain.

To illustrate the influence of different initial system states on the transition region, three levels of superheat $\Delta T_{sup} = 3$, 15 and 30 °C at atmospheric pressure have been selected. These corresponds to Jakob numbers of $Ja = 9$, 45 and 90, respectively. The respective growth characteristics are illustrated in Fig. 6. As indicated in the

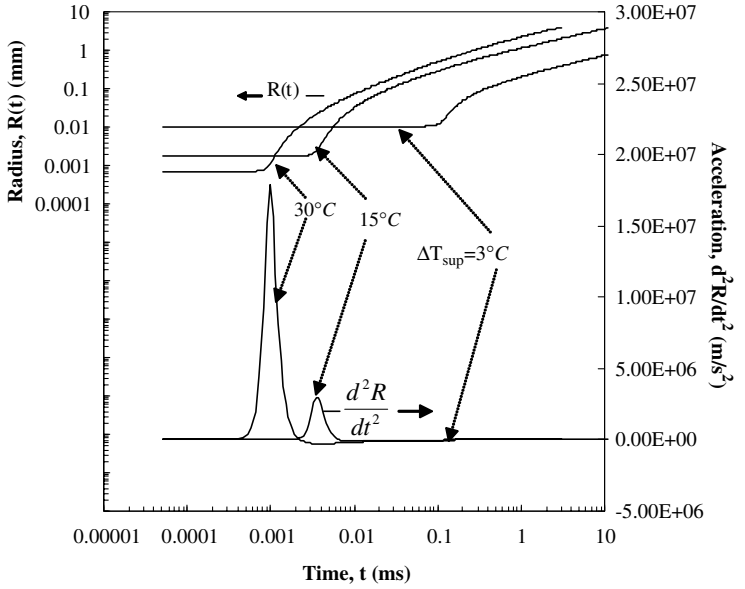

Fig. 6. Growth curves and interfacial acceleration for atmospheric pressure boiling and three levels of superheat $\Delta T_{sup} = 3$, 15 and 30 °C.

figure, the highest superheat case has the smallest initial radius as expected from Eq. (7). Since $(\partial P_v/\partial R)_{r=Rc} \propto (-1/R^2)$, the smaller R_c causes the rate of change of the vapour pressure to be higher such that a comparatively small increases in radius results in a disproportionately large decrease in the vapour pressure and temperature, P_v and T_v. As a consequence, a smaller initial radius means that a smaller increase in radius is required to produce a significant increase in the driving temperature for heat transfer $\Delta T(t)$. This is compounded by the fact that the initial penetration depth of the thermal layer was found to scale roughly as $\delta_0 \sim 1/3\ R_c$ such that the thermal resistance is smaller for smaller bubbles during this growth domain [8]. These factors have an important bearing on the thermal feedback effect which is responsible for accelerating growth in this region. For smaller initial bubble radii, the thermal feedback effect is intensified because a much smaller increase in radius is required to escalate the driving potential, $\Delta T(t)$. Consequently, the rate at which the temperature difference, interfacial heat flux and growth rate increase for the $\Delta T_{sup} = 30$ °C case is comparatively high and decreases for the $\Delta T_{sup} = 15$ °C and $\Delta T_{sup} = 3$ °C cases, respectively. This is signified by the magnitude and time of occurrence of the peak acceleration in Fig. 6, since $d^2R/dt^2 \propto d(\Delta T)/dt$.

Following this physical reasoning, an order of magnitude approximation for the delay time can be formulated by assuming that the time it takes for the thermal feedback effect to generate a significant driving temperature difference is related to the time it takes the system to react to a change in its thermal environment as characterized by a thermal time constant, t_c. With this assumption, the delay time was scaled as

$$t_c \approx \frac{L_c^2}{\alpha_l} = \frac{1}{9\alpha_l}\left(\frac{2\sigma}{P_{sat}(T_\infty) - P_\infty}\right)^2, \tag{21}$$

where the penetration depth is characterized by the length scale for a sphere, $L_c \approx \delta_0 \sim 1/3R_c$, and Eq. (7) has been substituted for R_c. Fig. 7 shows good qualitative agreement with this simple analysis and the predicted delay times for a significant range of initial system conditions for the numerical predictions of this work as well as those of Lee [7]. Changes in the magnitude of the

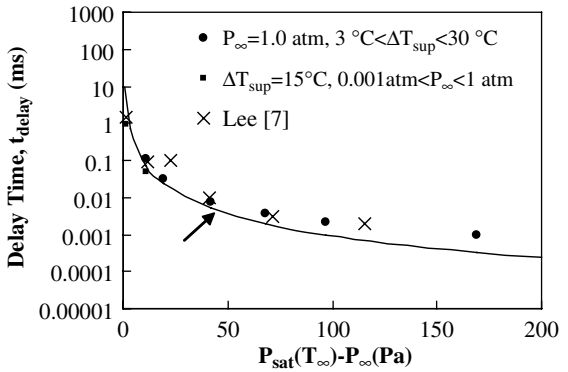

Fig. 7. Comparison of scaling analysis delay times and the computed delay times of the numerical simulations.

initial disturbance have an effect on the computed delay times but not as much as necessary to change the proposed order of magnitude argument presented above.

3.2.2. Effect of system properties on the transition domain

For inertial forces to play a major role during the transition domain, the thermal feedback effect must accelerate bubble growth to such an extent that the hydrodynamic force at the interface becomes large enough to influence the rate of change of the vapour pressure as it decreases from $\Delta P_{\max}$ to close to zero. The order of magnitude of the velocity which characterizes inertial limited growth can be represented by the Rayleigh formulation since the acceleration drops off quickly enough that $3/2\rho_l(dR/dt)^2 \gg \rho_l R(d^2R/dt^2)$ during the initial phase of the transition domain [8]

$$U_i \approx O\left(\sqrt{\frac{2}{3}\frac{P_{sat}(T_\infty)-P_\infty}{\rho_l}}\right)=\sqrt{\frac{4\sigma}{3\rho_l R_c}}. \tag{22}$$

The absolute maximum velocity that can be generated by the system is related to the maximum possible heat flux corresponding to $\Delta T_{\max}/\delta_{\min} \sim \Delta T_{sup}/\delta_0$, such that

$$U_{HT} \approx O\left(\frac{3\alpha Ja}{R_c}\right), \tag{23}$$

where the approximation $\delta_0 \sim 1/3R_c$ has been substituted. The ratio of the squares of these two characteristic velocities provides an indication of the inertial force required to influence the growth dynamics compared with the latent energy available to generate the inertial force

$$I_R \equiv \frac{U_i^2}{U_{HT}^2} = \left(\frac{4}{27}\right)\left(\frac{\sigma}{\rho_l\alpha^2}\right)\frac{R_c}{Ja^2}\begin{cases}\ll 1, & \text{Inertia controlled}\\ \gg 1, & \text{Diffusion controlled}\end{cases} \tag{24}$$

Fig. 8a shows the case for $Ja = 3167$ such that $I_R \ll 1$. Here the inertial force required to govern the growth process is much less than that available so that the hydrodynamic resistance increases to such an extent that a substantial pressure differential, $\Delta P_v(t) \sim \Delta P_{v_0}$, is sustained. In this way, the explosive growth that would have occurred if $\Delta T(t)$ increased to its maximum before the thermal boundary layer had sufficient time to grow is

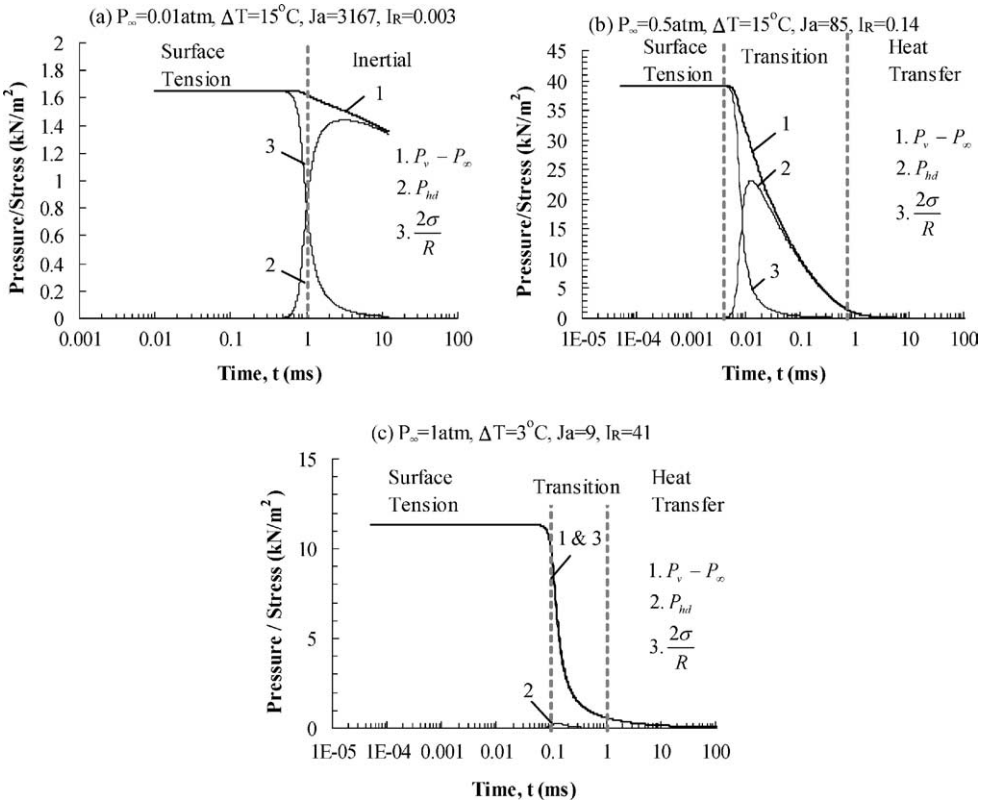

Fig. 8. Curves showing the varying influence of the hydrodynamic pressure in determining the rate of change of the vapour pressure for differing initial system condition.

averted. The calculated maximum velocity was $U_{max} = 0.976$ m/s which corresponds with $U_i = 1.05$ m/s, indicating that the Rayleigh solution offers an adequate approximation during the transition phase for $I_R \ll 1$ and growth can be considered inertia controlled. Conversely, Fig. 8c shows the case for $Ja = 9$ such that $I_R \gg 1$. Here the inertial force required to govern the growth process is much greater than that available so that the bubble is unable to generate the hydrodynamic resistance necessary to influence the growth process significantly. As a result, $\Delta T(t)$ increases at the highest possible rate so that the highest interfacial heat flux can be generated to sustain bubble growth. The calculated maximum velocity was $U_{max} = 0.42$ m/s which corresponds with $U_{HT} = 0.44$ m/s indicating that growth is diffusion limited for $I_R \gg 1$. Figs. 4 and 8b illustrate some intermediate cases, $Ja = 45$ and 85, respectively, in which the growing bubble generates sufficient inertia to influence $\Delta P_v(t)$, but not enough to be considered inertia limited as prescribed by the Rayleigh solution. Here, both the liquid inertia and thermal diffusion play important roles in determining the growth characteristics during the transition domain.

3.2.3. Effect of system properties on the heat transfer domain

Fig. 9 shows the temporal variation of the thickness of the thermal boundary layer, $\delta(t)$ for a variety of test cases. In this figure the individual curves have been shifted to the left by an amount of time prescribed by the respective delay times so that comparisons can be made between bubbles which begin growing at the same time. The figure indicates that for early growth, the curves are very different but converge quickly. Initially, the characteristic length scale which dominates the fluid flow and heat transfer is dictated by the initial radius of the bubble. This is confirmed by noting that the initial thermal layer thickness increases with initial bubble radius. However, each bubble expands at a rate which is much higher than the rate at which their respective thermal layer grows and a new length scale develops which is independent of the bubble radius since $\delta/R \ll 1$ for each bubble. This constitutes the thin thermal boundary layer which has been the subject of several studies as discussed earlier. Since the thermal diffusivity of water does not change considerably for the range of superheat and pressures tested the growth rate of the thermal boundary layer is not sensitive to changes in pressure or superheat In this way, differences in the magnitude of the growth rate during the heat transfer domain for different system states depend on the initial superheat and the density ratio as defined in the Jakob number.

4. Revisiting the MRG solution

The numerical solutions of the present study provide some justification for the physical modelling of the MRG formulation for predicting the growth characteristics during the transition phase from moderate to high Jakob numbers as well as indicating why the MRG formulation is not valid during this domain for low Jakob numbers. The MRG formulation assumes that the rate of change of the vapour pressure is governed by hydrodynamic forces in such a way that the equation

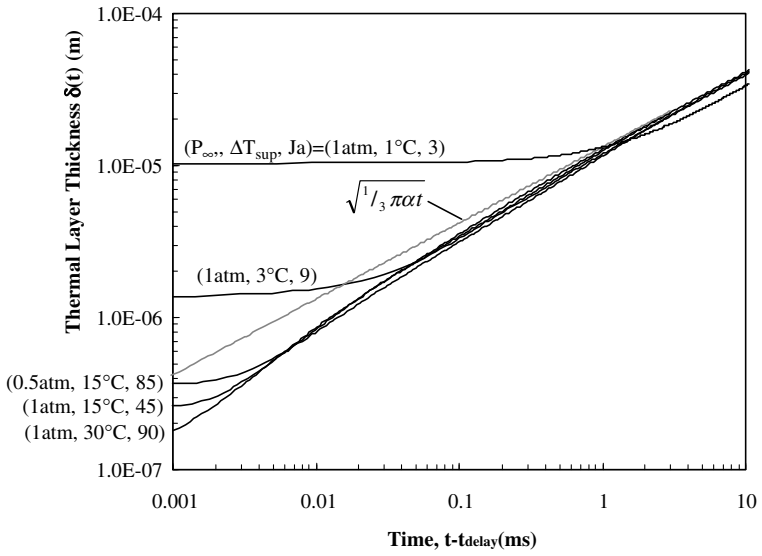

Fig. 9. Growth of the thermal boundary layer for different initial system conditions.

of motion simplifies to the following expression for the interfacial velocity

$$\frac{dR}{dt} \approx \sqrt{\frac{2}{3}\left(\frac{\Delta P_v(t)}{\rho_l}\right)}. \quad (25)$$

Secondly, the analysis requires the thin thermal boundary layer assumption be applicable so that the interfacial energy balance simplifies to

$$\frac{dR}{dt} \approx \frac{k_l}{\rho_v h_{fg}}\left(\frac{\Delta T_v(t)}{\sqrt{\pi/3\alpha t}}\right). \quad (26)$$

Assuming a linear variation of $\Delta T(t)$ with $\Delta P_v(t)$, equating the two expressions above gives a quadratic expression for $\Delta T(t)$. Substituting the positive root of the quadratic equation into either Eqs. (25) or (26) and integrating gives an approximation for the instantaneous bubble radius

$$R(t) - R_c = \frac{2}{3}C_0\left[(t+4C)^{3/2} - t^{3/2} - (4C)^{3/2}\right],$$
$$C = \frac{9\rho_l \alpha Ja^2}{2\pi\Delta P_{v_0}}, \quad C_0 = \sqrt{\frac{\pi}{27\alpha}}\left(\frac{\Delta P_{v_0}}{\rho_l}\right)\frac{1}{Ja}. \quad (27)$$

If the Clapeyron equation is substituted to relate the initial pressure differential $\Delta P_{v_0} = P_{sat}(T_\infty) - P_\infty$ to the system superheat, ΔT_{sup}, rearranging Eq. (27) gives the MRG solution equations (5) and (6). To circumvent any problems inherent in utilizing the Clapeyron equation, the above formulation is plotted in Fig. 10 using accurate values of $P_{sat}(T_\infty)$ and compared with the computed growth curves for a range of Jakob numbers. The figure indicates that provided that the Jakob number is large enough, the MRG-type formulation does a very good job at predicting the computed growth curves for the transition phase as indicated by the portion of the curves with a slope greater that 1/2. This is not the case for low Jakob numbers ($Ja < 10$). One reason for the discrepancy for low enough Jakob numbers is that

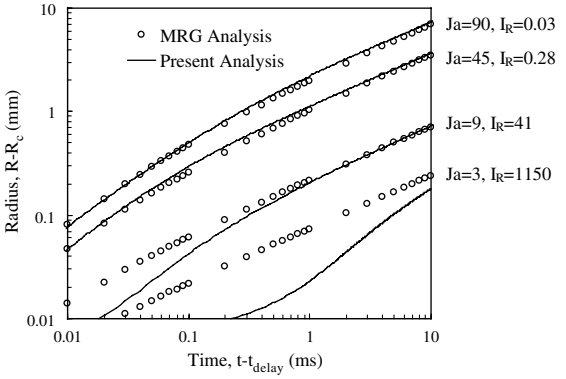

Fig. 10. Comparison of MRG-type formulation, Eq. (27), with present analysis.

the inequality $(U_i/U_{HT})^2 = I_R \gg 1$ holds true so that the vapour pressure is governed by surface tension, $\Delta P_v(t) \approx 2\sigma/R(t)$, not the hydrodynamic pressure. Hence, the assumption implicit in the MRG solution is incorrect and the solution should not give valid results during the transition phase. For higher Jakob numbers, the inequality $(U_i/U_{HT})^2 = I_R \gg 1$ does not hold true so that the agreement should improve with increasing Jakob number as is indicated in the figure. Secondly, the analysis demands that the thin thermal boundary layer assumption be applicable. The validity of this assumption for higher Jakob numbers is confirmed considering that Fig. 9 shows that once the transition region commences, the thermal boundary layer thickness approaches the analytic solution, $\delta(t) \approx (1/3\pi\alpha t)^{1/2}$, within approximately 0.0045 ms for $Ja > 10$. For lower Jakob numbers ($Ja < 10$) it takes much longer for the thermal layer to approach the thin thermal layer solution which indicates that the MRG-type interpolation formulation will give progressively less accurate predictions during the transition phase of growth as the Jakob number is reduced.

5. Conclusions

The complicated thermal and hydrodynamic interactions between the vapour and liquid have been manifested for single isolated bubbles growing in an unbounded liquid from inception to fully heat transfer limited growth for a range of initial system conditions. It has been shown that early bubble growth from the initial radius is controlled by surface tension forces within the bubble wall and depends strongly on the initial critical bubble radius. Minuscule increases in radius result in an increase in the local interfacial temperature gradient which facilitates growth by increasing the heat flux into the bubble. If there is sufficient latent energy in the system, bubble growth becomes influenced by the fact that it now must force the surrounding liquid out radially. Nevertheless, the growth rate must eventually decrease with increasing time as the thermal energy stored within the boundary layer which surrounds the bubble is consumed by the bubble. Eventually the growth rate slows enough the liquid hydrodynamics no longer play an important role and the growth rate becomes limited by the rate at which the thermal boundary layer grows which dictates the rate that energy can be transported to the interface through the liquid.

References

[1] L. Rayleigh, On the pressure developed in a liquid during the collapse of a spherical cavity, Philos. Mag 34 (1917) 94–98.

[2] M.S. Plesset, S.A. Zwick, The growth of vapor bubbles in superheated liquid, J. Appl. Phys. 25 (1954) 493–500.
[3] H.K. Forster, N. Zuber, Growth of vapor bubbles in superheated liquid, J. Appl. Phys. 25 (1954) 474–478.
[4] L.E. Scriven, On the dynamics of phase growth, Chem. Eng. Sci. 10 (1959) 1–13.
[5] J. Riznic, G. Kojasoy, N. Zuber, On the spherically symmetric phase change problem, Int. J. Fluid Mech. Res. 26 (1999) 110–145.
[6] Y.C. Lien, Bubble growth rates at reduced pressure, D.Sc. Thesis, MIT, 1969.
[7] H.S. Lee, Vapour bubble dynamics in microgravity, Ph.D. Thesis, University of Michigan, 1993.
[8] A.J. Robinson, Bubble growth dynamics in boiling, Ph.D. Thesis, McMaster University, Hamilton, Ontario, Canada, 2002.
[9] P. Dergarabedian, The rate of growth of vapour bubbles in superheated water, J. Appl. Mech. 20 (1953) 537–574.
[10] B.B. Mikic, W.M. Rohsenow, P. Griffith, On bubble growth rates, Int. J. Heat Mass Transfer 13 (1970) 657–665.
[11] A. Prosperetti, M.S. Plesset, Vapour-bubble growth in a superheated liquid, J. Fluid Mech. 85 (1978) 349–368.
[12] T.G. Theofanous, L. Baisi, H.S. Isben, H. Fauske, A theoretical study on bubble growth in constant and time-dependent pressure fields, Chem. Eng. Sci. 24 (1969) 885–897.
[13] A.M. Judd, Analysis of transient boiling of liquid metals, Br. J. Appl. Phys. 2 (1969) 261–274.
[14] S.J. Board, R.B. Duffy, Spherical vapour bubble growth in superheated liquids, Chem. Eng. Sci. 26 (1971) 263–274.
[15] M. Dalle Donne, M.P. Ferranti, The growth of vapour bubbles in superheated sodium, Int. J. Heat Mass Transfer 18 (1975) 477–493.
[16] H.S. Lee, H. Merte Jr., Spherical vapour bubble growth in uniformly superheated liquids, Int. J. Heat Mass Transfer 39 (1996) 2427–2447.
[17] W. Chen, R. Mei, J.F. Klausner, Vapor bubble growth in highly subcooled heterogeneous boiling, in: Convective Flow Boiling Conference, Paper II-4,1995.
[18] A.J. Robinson, R.L. Judd, Bubble growth in a uniform and spatially distributed temperature field, Int. J. Heat Mass Transfer 44 (2001) 2699–2710.